Chemical Engineering Science 84 (2012) 188–196

Contents lists available at SciVerse ScienceDirect

Chemical Engineering Science

journal homepage: www.elsevier.com/locate/ces

Effect of bud scars on the mechanical properties of *Saccharomyces cerevisiae* cell walls

R.D. Chaudhari [1], J.D. Stenson [2], T.W. Overton, C.R. Thomas *

University of Birmingham, School of Chemical Engineering, Edgbaston, Birmingham B15 2TT, United Kingdom

HIGHLIGHTS

- Freshly grown *S. cerevisiae* cells were sorted by number of bud scars using FACS.
- Mechanical properties of the sorted cells were found by compression testing.
- 69% of cell walls were linear elastic to bursting but only 32% of daughter cells.
- Scars caused mechanical property differences between daughter and mother cells.

ARTICLE INFO

Article history:
Received 8 June 2012
Received in revised form
13 August 2012
Accepted 17 August 2012
Available online 25 August 2012

Keywords:
Cellular biology and engineering
Mathematical modelling
Elasticity
Yeast
Alexa Fluor 488 wheat germ agglutinin
Fluorescence activated cell sorting

ABSTRACT

To determine the effect of bud scars on the mechanical properties of the walls of *Saccharomyces cerevisiae* cells, freshly cultivated stationary phase cells stained with Alexa Fluor 488 conjugated wheat germ agglutinin were sorted according to the number of bud scars using fluorescence-activated cell sorting (FACS). The groups were daughter cells with no bud scars, and mother cells separated further by number of scars (one, two and more than two). Cells with more than three scars were very rare.

Compression testing by micromanipulation was used to determine key mechanical properties of the sorted cells. For all cells the force and fractional deformation at bursting could be determined. For 69% of cells overall but only 32% of daughter cells, a large strain mathematical model using a linear elastic constitutive equation for the wall material could be fitted to force deformation data up to cell wall failure. For these cells, the wall surface modulus, elastic modulus, initial stretch ratio and strain energy per unit volume at bursting could be estimated. For the remainder of the cells, the lack of permanent deformation on repeated compression and release (at deformations not causing bursting) suggested the cell wall material was non-linear elastic but with no observable plastic behaviour.

This is the first report to show directly that bud scars affect the global mechanical properties of yeast cells and that the important distinction with respect to scars is between daughter and mother cells. The former were smaller with more elastic walls and a higher mean initial stretch ratio. For cells for which the model could be fitted, the mean circumferential strain at bursting decreased with scarring (consistent with stiffer walls) whilst the stress increased. This may be due to the reported absence of chitin in the walls of daughter cells.

© 2012 Elsevier Ltd. Open access under CC BY license.

1. Introduction

Compression testing by micromanipulation has been used to measure mechanical properties of single *Saccharomyces cerevisiae* cells (Mashmoushy et al., 1998; Smith et al., 1998, 2000a, 2000b; Stenson et al., 2009, 2011). In this technique a single cell is compressed between two flat surfaces and the force required to deform and burst it and the deformation at bursting measured directly. However, the bursting force and deformation are not intrinsic mechanical properties of the cells as they depend on the measurement method e.g., the speed of compression. Using a suitable mechanical model of the cell wall, more fundamental properties such as the cell wall elastic modulus can be derived (Smith et al., 2000a; Stenson et al., 2009, 2011). In particular, Stenson et al. (2009) modelled the large strains found in yeast cell walls at high deformations using a linear elastic cell wall constitutive equation. These workers also used fast compressions so that time dependent effects such as water loss from cells could be neglected. This allowed the initial stretch ratio of each cell as well as its wall elastic modulus to be found. The initial stretch ratio is the

* Corresponding author. Tel.: +44 121 4145355; fax: +44 121 4145434.
E-mail address: c.r.thomas@bham.ac.uk (C.R. Thomas).
[1] Present address: Biochemical Engineering Unit, Chemical Engineering & Process Development Division, National Chemical Laboratory, Dr. Homi Bhabha Road, Pune 411 008, India.
[2] Present address: Malvern Instruments, Enigma Business Park, Malvern, Worcestershire, WR14 1XZ, UK.

0009-2509 © 2012 Elsevier Ltd. Open access under CC BY license.
http://dx.doi.org/10.1016/j.ces.2012.08.027

cell diameter at the start of compression divided by that at zero turgor pressure and is important as it reflects the initial strain in the walls. It was shown that the model fitted force deformation data for reconstituted dried yeast cells up to cell wall failure (cell bursting). It was therefore possible to estimate cell wall failure criteria such as the strain energy per unit wall volume at failure.

Using this method and model, it has been shown that the mean elastic modulus for rehydrated dried Baker's yeast cells was 185 ± 15 MPa, the mean initial stretch ratio was 1.039 ± 0.006, the mean circumferential stress and strain at failure were 115 ± 5 MPa and 0.46 ± 0.03, respectively, and the mean strain energy per unit wall volume at failure was 30 ± 3 MPa (Stenson et al., 2011).

In all modelling to date, it has been assumed that the yeast cell wall is homogenous, has uniform thickness and that the wall thickness to cell radius ratio remains constant (i.e., wall thickness increases with cell diameter). However, the yeast cell wall is a continuous three-dimensional elastic structure (Klis et al., 2006; Lesage and Bussey, 2006) that can vary in composition and structure depending upon mode of cultivation, growth conditions and cell age (Aguilar-Uscanga and Francois, 2003; Bitterman et al., 2003; Powell et al., 2000, 2003; Sinclair et al., 1998; Werner-Washbourne et al., 1993). It is known that cell walls thicken as batch cultures enter the stationary phase (Bitterman et al., 2003; Werner-Washbourne et al., 1993). One aspect of ageing is the appearance of scars in the cell wall during the budding process by which *S. cerevisiae* divides. During cytokinesis a prominent chitinaceous scar forms on the mother cell (the bud scar, occupying around 1–2% of the cell surface) and a corresponding birth scar forms on the daughter cell, occupying around 5% of the surface area (Bitterman et al., 2003; Powell et al., 2003; Sinclair et al., 1998; Werner-Washbourne et al., 1993). Ageing in yeast cells is not defined by the chronological lifespan of a cell but by its replicative age as indicated by the number of these bud scars on the cell wall (Bitterman et al., 2003; Powell et al., 2003). Although yeast cells can have as many as 20 bud scars, this study focussed primarily on cells with up to 3 such scars because cells with more than this are rare in normal culture. This permitted a comparison between daughter and mother cells. However, few if any of the cells could be described as senescent; this was not an ageing study.

Although nano-indentation by atomic force microscopy has been used to study the local mechanical properties of bud scars (Arfsten et al., 2010; Touhami et al., 2003) there is no information on the effect of scarring on overall yeast cell mechanical properties, which might be important in understanding yeast bioprocessing. Compression testing by micromanipulation (Stenson et al., 2009, 2011) was used for this purpose in this work. However, it is not possible to identify bud scars on the surface of the cells under compression with existing equipment. It was therefore necessary to sort the cells with respect to the number of bud scars, using a new method, in which scars were stained with Alexa Fluor 488 conjugated wheat-germ agglutinin (WGA-Alexa488) and sorted using a fluorescence activated cell sorter (FACS). WGA binds specifically to *N*-acetyl-glucosamine, the major component of chitin present in bud scars but binds only weakly with chitin elsewhere in the cell wall (Yamamoto et al., 1981). FITC-labelled WGA has been used previously to study bud scar numbers and morphology (Bitterman et al., 2003; Chen et al., 2003; Yamamoto et al., 1981) but WGA-Alexa488 has the advantage of superior photostability and a greater conjugate fluorescence.

2. Materials and methods

2.1. Yeast fermentation and sample preparation

Baker's yeast (*S. cerevisiae*; Fermipan Red, DSM Bakery Ingredients, Dordrecht, Holland) was chosen as it has been used in previous studies. A cell bank was generated to ensure consistency throughout the study. Yeast cells rehydrated in phosphate buffered saline (PBS) were cultivated on YM agar plates ($3\ g\ L^{-1}$ yeast extract, $3\ g\ L^{-1}$ malt extract, $5\ g\ L^{-1}$ peptone and $10\ g\ L^{-1}$ dextrose) at 30 °C for 24 h. Yeast colonies were harvested, washed in PBS (Oxoid; pH 7.3 at 25 °C), resuspended in stock solution ($250\ g\ L^{-1}$ glycerol, $10\ g\ L^{-1}$ yeast extract, $20\ g\ L^{-1}$ peptone) and stored in 1 mL aliquots at −80 °C. Yeast cultures were grown in 40 mL YPD medium ($10\ g\ L^{-1}$ yeast extract, $20\ g\ L^{-1}$ peptone and $20\ g\ L^{-1}$ glucose, adjusted to pH 5 using 2 M hydrochloric acid) in 500 mL conical flasks at 30 °C and 260 rpm for 24 h. Flasks were inoculated with 1 mL of the cell bank. This protocol was designed to obtain consistent batches of fresh yeast cells having similar properties throughout the study. Biomass accumulation was monitored using optical density at 550 nm, dry cell weight by drying 5 mL samples for at least 12 h at 105 °C and direct cell counting using a haemocytometer. Cell viability was checked using methylene blue; a 1:1 mixture of cell suspension and methylene blue solution ($0.2\ g\ L^{-1}$) was examined by optical microscopy after 1 min. Cells were harvested during stationary phase (ca. 24 h), stored in PBS at 4 °C and were used in compression tests within 48 h. There was no significant change in cell diameter and deformation and force at failure during this time (data not shown). It was shown that stationary phase samples contained a relatively low percentage of budded cells (exponential phase $79 \pm 2\%$, stationary phase $18 \pm 3\%$), which made these samples most suitable for compression testing. As described later, about half the cells in each sample were daughter cells, providing two roughly equal populations for comparison of daughter and mother cells.

2.2. Cell size and initial stretch ratio measurement by Mastersizer^{TM}

Cell size is a parameter required for modelling cell wall mechanical behaviour. The mean population values found by compression testing were validated by comparison with cell size distributions found using a Malvern Mastersizer 2000 (Malvern Instruments, Worcestershire, UK). Mild sonication was used to detach daughter cells from budding, stationary phase, mother cells before analysis. For each sample, 20 mL of cell suspension were sonicated on ice using a Status US70 probe (Philip Harris Scientific, UK) for 30 s at 65% power. 0.5 mL (at ca. 1.2×10^7 cells mL^{-1}) were then mixed into 100 mL of water and allowed to equilibrate for 1 min before the size distribution was determined (10^4 measurements). The refractive index of yeast was taken as 1.53 and the absorbance 0.1 (Smith et al., 2000b). Mastersizer measurements are fundamentally volume distributions. Assuming cells are spheres allows the equivalent spherical diameter of a cell to be found from its volume. Although the sphericity assumption may introduce systematic error, this was necessary for size comparisons with equivalent data from optical microscopy and compression testing.

The initial stretch ratio is the ratio of the cell volume at a given osmotic pressure to the volume of the cell at zero turgor pressure (when the internal and external osmotic pressures are equal). It is a fitted parameter of the modelling. However, it may also be determined from cell size measurements at different external osmotic pressures, here by Mastersizer. Nine sodium chloride solutions of osmotic pressures between 0.4 and 25 MPa were prepared. 0.5 mL of suspension at ca. 1.2×10^7 cells mL^{-1} were mixed into each solution in turn and allowed to equilibrate for 1 min before the cell volume distribution was determined (10^4 measurements). The equipment was cleaned twice with distilled water between determinations. The mean initial stretch ratio was determined for the whole population, not cells sorted by number

of scars, because individual cell initial stretch ratios were found by compression testing, as described later.

2.3. Initial stretch ratio measured by visualization chamber

The initial stretch ratio was also measured by direct observation of the effect of external osmotic pressure changes on individual cells using a visualization chamber (Berner and Gervais, 1994; Stenson et al., 2011). The construction and operation of the visualization chamber is described elsewhere (Stenson et al., 2011). Yeast cells were fixed to the bottom plate of the chamber using chitosan (Fluka, Biochemika, Switzerland, No. 22741) which has been shown to have no detrimental effect on yeast cells (Champluvier et al., 1989). The top plate of the chamber was placed in position and the chamber was sealed. Nine sodium chloride solutions of osmotic pressures between 0.4 and 25 MPa were prepared and starting from lowest osmotic pressure, the chamber was filled with solution and 1 min was allowed for cells to change volume before the solution was replaced with the next highest in osmotic pressure. Images were captured through a microscope at 400 × magnification and were analysed to obtain the dimensions of the cells using a QWin image analyser (Leica Microsystems Ltd, Milton Keynes, UK). Most cells were approximately prolate ellipsoids and this was assumed in calculating cell volumes from major and minor axis lengths. Assuming geometric similarity between uninflated (zero turgor) and inflated cells, the initial stretch ratio (λ_s) of a cell can be calculated from Eq. (1):

$$\lambda_s = \left(\frac{V}{V_0}\right)^{\frac{1}{3}} \tag{1}$$

where V is the volume of cell in PBS and V_0 is the volume of the cell at zero turgor. At external osmotic pressures higher than the point of zero turgor, cells were presumed to behave as ideal osmometers obeying the Boyle van't Hoff relationship (Nobel, 1969). This means that the volume at zero turgor can be found from a plot of volume against the reciprocal of the external osmotic pressure, as described in detail elsewhere (Stenson, 2008; Stenson et al., 2011). The equivalent spherical diameter was again found from the volume.

Cells with different numbers of scars were not tested independently because this is a very time consuming process.

2.4. Fluorescent microscopy and cell sorting

2.4.1. Fluorescent microscopy

Bud scars and birth scars were fluorescently labelled using Alexa Fluor 488 conjugated wheat germ agglutinin (WGA-Alexa-488; Molecular Probes, Inc; excitation 495 nm and emission 519 nm).

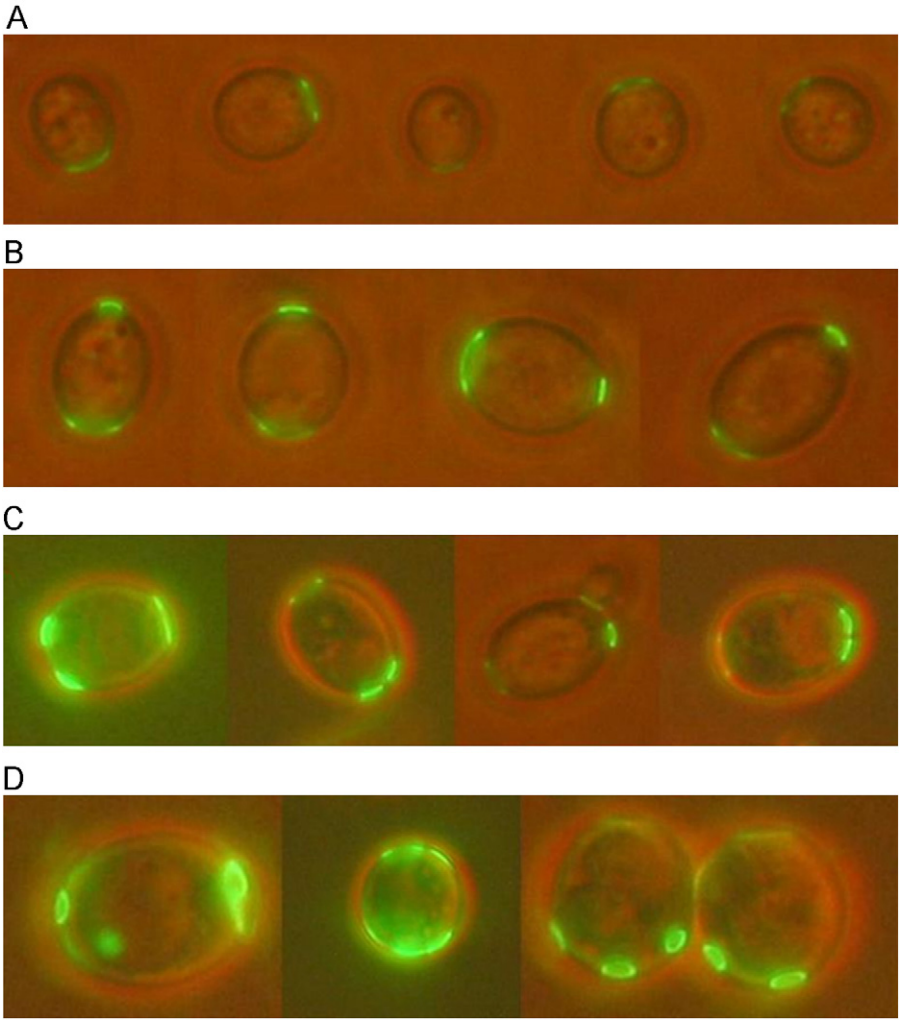

Fig. 1. Images of yeast cells stained with Alexa Fluor 488 conjugated wheat germ agglutinin captured by fluorescent microscopy with low intensity visible light in the background. (Images not to scale, magnification in each case greater than 100 ×). (A) Daughter cells having only a birth scar; (B) cells with a single bud scar; (C) cells with two bud scars; and (D) cells with three or more bud scars. It was not always possible to capture a clear image of all scars present on the surface of a cell but these were observable by fine focus changes.

A volume of 1 mL of yeast cell suspension in PBS was incubated with 13 μL of WGA-Alexa 488 (1 mg mL^{-1}) at room temperature in the dark for 60–90 min with and gentle mixing every 15 min. Before use, cells were washed with PBS at least twice to remove excess dye. Cells were visualised by fluorescent microscopy (Leica Microsystems Ltd., UK, mercury arc excitation, filter set 480–520 nm). Examples are shown in Fig. 1. The number of scars on each cell could be identified. Both bud and birth scars were clearly visible. Daughter cells had a distinct birth scar, bigger in size than a bud scar but of relatively low fluorescent intensity. Cells with one bud scar were found to have the scar directly opposite the birth scar (Fig. 1B). Two bud scars on a cell were beside one another opposite the birth scar (Fig. 1C) whereas there seemed to be no preferred pattern for cells with more than two scars (Fig. 1D). These patterns have been observed previously (Freifelder, 1960). It was possible to use these patterns to confirm direct counts of the number of scars.

The cells appeared to be prolate ellipsoids. The major and minor axis lengths of the cells were measured using a QWin image analyser (Leica Microsystems Ltd, UK) and the equivalent diameter of each cell was calculated. The number mean equivalent diameter of the whole population was calculated and compared with that from the visualization chamber.

2.4.2. Fluorescence activated cell sorting (FACS)

WGA-Alexa488 stained yeast cells were sorted according to bud scar number using a FACSAria2 Cell Sorter (BD Biosciences, UK). Particles were excited with a 488 nm blue laser and fluorescence was detected using a 530/30 nm bandpass filter and 502 nm longpass mirror. Single cells were first identified using forward scatter and side scatter height-versus-width plots. These were than sorted by fluorescence intensity into four populations, corresponding to daughter cells (low green fluorescence, no bud scars), and cells with one, two or three or more bud scars (increasing green fluorescence). Cells were sorted into PBS using the purity sort mode. Fluorescence microscopy was used to check that each sorted group contained mainly or entirely cells with the expected number of bud scars. The purity of each group was determined by observing a random selection of 50 cells in each case.

2.5. Cell wall thickness measurement by using transmission electron microscopy (TEM)

Calculation of mechanical properties such as the cell wall elastic modulus requires knowledge of the cell wall thickness. This cannot be determined for individual cells during compression testing so a mean value is used, usually expressed as the ratio of wall thickness to cell radius, τ (Smith et al., 2000b). In this study τ was determined for cells with different numbers of bud scars. Samples of sorted cells were incubated in 500 μL of 2.5% glutaraldehyde primary fixative solution for 2 h at room temperature. Secondary fixation was with 1% osmium tetroxide, followed by sequential dehydration with ethanol and propylene oxide and then resin embedding under vacuum. The embedded cells were sectioned, re-stained with pure resin and photographed at magnifications from $\times$10,000 to $\times$80,000 using a Jeol 1200 EX TEMSCAN (Jeol UK Ltd, Welwyn Garden City, UK). Cross-sectional areas of the cytoplasm and wall of randomly chosen cells were analysed using a QWin image analyser (Leica Microsystems Ltd, Milton Keynes, UK). A sample image is shown in Fig. 2.

TEM sectioning cuts cells at random distances from the equator and therefore the diameter and cell wall thickness measured from the images must be corrected. In previous work (Smith et al., 2000b; Stenson et al., 2011) the correction of Smith et al. (2000b) was used but this method has been questioned recently for microcapsules (Mercadé-Prieto et al., 2011). A revised method of obtaining the mean value of τ was used in this study and this is provided in the Supplementary information.

2.6. Compression testing of yeast cells by micromanipulation

The basic principle of the micromanipulation technique is to compress a single cell between two parallel and fixed surfaces until it bursts (Mashmoushy et al., 1998). The method followed that of Stenson et al. (2011) in which cells are compressed between a (50 μm diameter) glass probe and the bottom of a glass chamber containing the cell suspension. The compression speed was 68 μm s^{-1}. A 406A force transducer (Aurora Scientific Inc., Ontario, Canada) was used to measure force during compression. This gave a better noise to signal ratio than the 403A transducer used previously. The voltage output from the transducer was recorded by an Amplicon PCI 120 data acquisition card (Amplicon Liveline Ltd., Brighton, UK) which has a resolution of 0.00488 V over a full scale of ca. $\pm$10 V. The data capture rate was 1000 s^{-1}. The compliance of the transducer and probe was 10 μm mN^{-1}. Force versus time data were converted to force versus probe displacement using the speed of compression and then to force versus fractional deformation using the compliance and the cell diameter. The latter could be found from the force data. It was strictly the (initial) length of the minor axis of the cell, although cells were treated as spherical in the analysis, as discussed later. Fig. 3 shows typical compression data. The fast compression rate and restricted data capture rate resulted in relatively small data sets, although these were adequate for later analysis. Twenty five cells could be characterised per hour and each sample was characterised within 1.5 h of sampling.

In previous studies (Smith et al., 2000b; Stenson et al., 2009, 2011) it had been found that rehydrated, stationary phase yeast cell walls were elastic up to failure (cell bursting). This was confirmed here to high fractional deformations by repeat

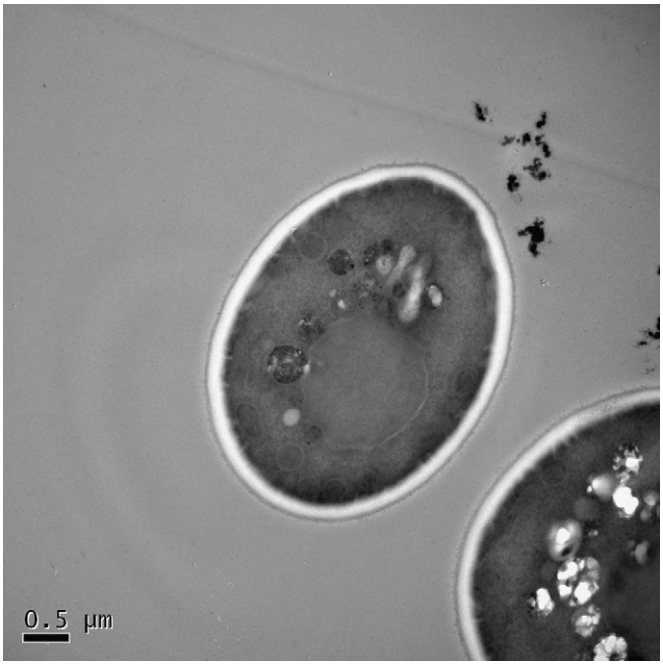

Fig. 2. A typical transmission electron microscopy section of a yeast cell with a wall approximately 200 nm thick ($\times$20,000).

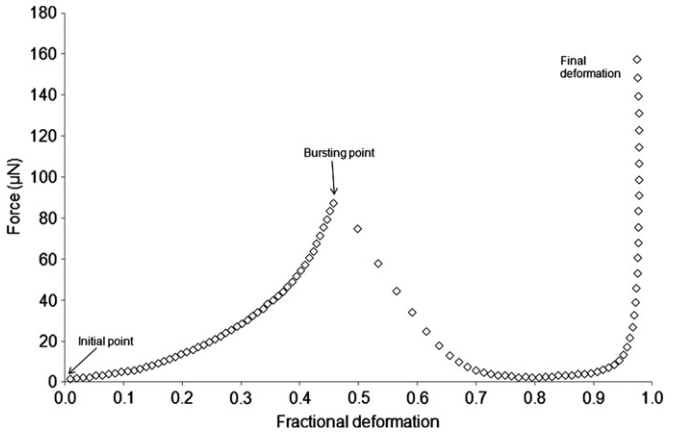

Fig. 3. A typical example of a force–deformation curve for a 5.1 μm yeast cell. Compression speed 68 μm s^{-1}. Data capture rate 1000 s^{-1}.

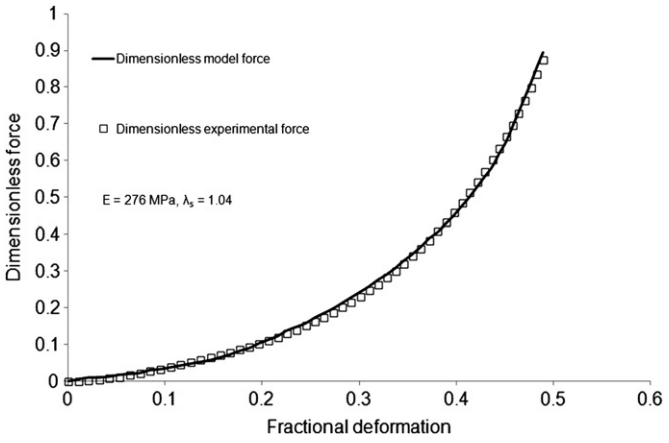

Fig. 4. A typical example of a best fit of the mechanical model to experimental cell compression data. The model was that of Stenson et al. (2009) in which it was assumed that the cell wall material was linear elastic. Simulations of compressions were done using the elastic modulus E and the initial stretch ratio λ_s as adjustable parameters. Simulated and experimental force–deformation data were converted to dimensionless form for fitting using a least square method to find the best fit (Stenson et al., 2009).

compression-release experiments in which no permanent deformation was observed (data not shown).

2.7. Modelling compression testing data

Force deformation data obtained from compression testing cannot be used directly to estimate the elastic modulus of yeast cell walls. An analytical model has been developed to describe the compression of a single yeast cell between parallel flat surfaces (Stenson et al., 2009). In this model the cells are considered as liquid filled, thin walled spheres compressed to bursting at such high compression rates that water loss during compression might be neglected. The cell wall material was assumed to be linear elastic i.e., to have a linear elastic constitutive equation, although the model itself was non-linear due to geometrical factors and the high strains and rotations found in the wall during compression (Stenson et al., 2009). Using the model, cell compression was simulated in MATLAB™ (Mathworks INC, USA) with two adjustable parameters i.e., the elastic modulus and the initial stretch ratio. It was not possible to determine the latter for individual cells during compression tests (for example by changing the osmotic pressure of the suspension as in Section 2.3) because of equipment limitations and time constraints. The elastic modulus and the initial stretch ratio were the adjustable parameters used in previous work (Stenson et al., 2009, 2011). The governing equations of the model were solved using the Runge–Kutta method with the MATLAB ode45 solver (Wang et al., 2006; Stenson et al., 2009). Assuming time independence, each simulation was solved as a series of static equilibrium problems with increasing steps of probe displacement i.e., cell deformation. Force–deformation data, whether simulated using the model or found by experiment were converted to dimensionless form to simplify the fitting process (Smith et al., 2000b; Stenson et al., 2009). A least square method was used to choose the values of initial stretch ratio and elastic modulus that gave the best fit of model to experimental data. The semi-automatic fitting procedure was implemented in a MATLAB program. Although this program could indicate the initial point of the compression (when probe touched the cell), the bursting point and the point at which the cell reached the chamber base, there was always manual confirmation or correction of these points before fitting began. This was necessary because of artefacts caused by noise. The key points are shown for the example in Fig. 3 and the corresponding fit in Fig. 4.

2.7.1. Fitting the model to experimental data

Although it appeared from control experiments that most if not all cells were elastic up to bursting (no observations of irreversible plastic behaviour), fitting a model assuming a linear elastic cell wall material failed on about 31% of the cells overall and 68% of daughter cells. This was indicated by the initial stretch ratio appearing to be outside the reasonable range of 1.00 to 1.15 determined by visualization chamber data, as shown later. Fig. 5 shows an example of such a failed attempt. In such cases the quality of fitting was not greatly improved by any physiologically reasonable adjustment to the initial stretch ratio. Lacking a suitable model using non-linear elastic cell walls, it was decided to fit the model only to those cells that showed linear elastic wall behaviour to failure. The possibility of fitting the model only to low strain data (as has been done for plant cells; Wang et al., 2006) was rejected, as there appeared to be no reliable method to select the higher strain data to be excluded. The relatively fast compression speeds and therefore low number of points in the force deformation data exacerbated this situation by making the fitting parameters dependent on the amount of data included.

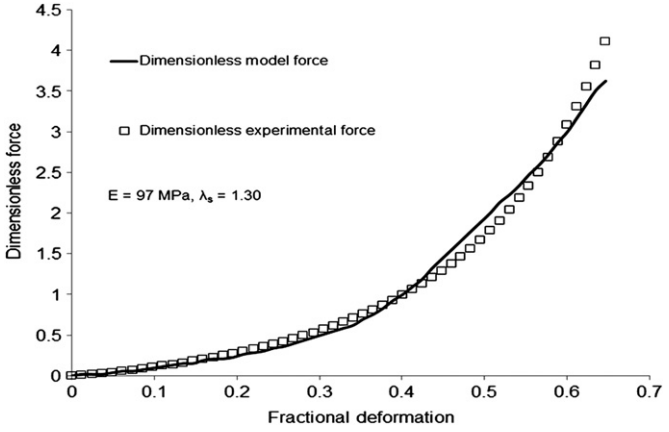

Fig. 5. A typical example of a failed attempt to fit the model of Stenson et al. (2009) to cell experimental compression data. The initial stretch ratio λ_s was permitted to take values from 1.00 to 1.30 in steps of 0.01 and the elastic modulus E from 50 to 300 MPa in steps of 1 MPa. The best fit was with λ_s=1.30, which is a physiologically unrealistic value.

Where cells could be fitted up to bursting, the failure criteria of strain energy per unit wall volume and circumferential stress and strain were found (Stenson et al., 2009).

3. Results and discussion

3.1. Cell viability

The stationary phase cells selected for compression testing had a viability of about 98%. The viability of cells resuspended in PBS remained as high as 95% after 3 weeks at 4 °C. This could reflect the commercial source of the strain that may have been selected for its stability. The robustness of this cell line makes it particularly suitable for compression testing, which is a relatively slow analytical technique. Nevertheless, all compression testing was done within 48 h of cell harvest.

3.2. Cell sizes by Mastersizer

Mild sonication was effective in separating daughter cells from budding mother cells, resulting in a significant mean size reduction with time. After 30 s, less than 5% budded cells remained with no significant change in sample viability. Sonication for longer than 30 s did not significantly decrease the percentage of budded cells but after 60 s cell viability decreased. The highest number of single cells was at 30 s so this was the chosen protocol. The volume distribution obtained from these cells was transformed to a number distribution giving a mean value of 5.07 ± 0.04 μm. This value did not change significantly on cell storage over 3 weeks at 4 °C.

3.3. Initial stretch ratios

Fig. 6 shows an example of data obtained from a visualization chamber experiment allowing the initial stretch ratio of an individual cell to be determined. The viability of cells fixed to the visualization chamber was approximately 80% immediately after fixation. The initial stretch ratio was only found for viable cells. The mean initial stretch ratio found to be 1.10 ± 0.01 (95% confidence limits; 20 cells). This is higher than the value of 1.033 ± 0.008 found previously for the same strain (Stenson, 2008). However, in previous work the cells were rehydrated from a dried state rather than cultured. It is quite likely that drying causes significant changes to yeast cell membranes and walls, with consequential effects on initial stretch ratios, although that was not tested here. The initial stretch ratio for an individual cell was as high as 1.15. The initial stretch ratio was independent of cell diameter (data not shown).

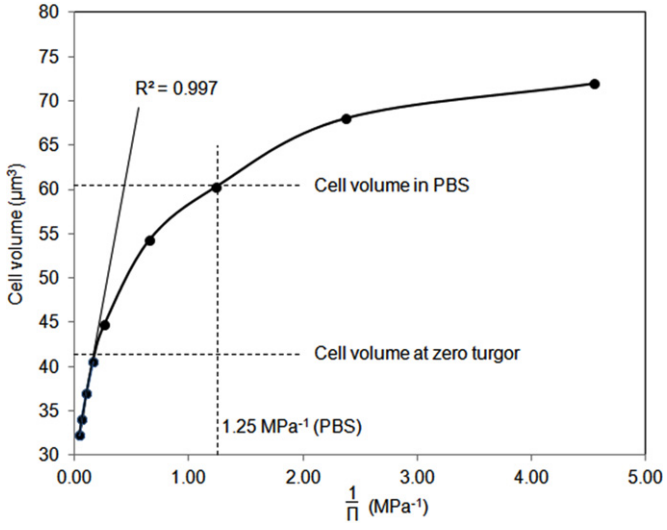

Fig. 6. An example of visualization chamber data showing the change in volume of a cell with changing external osmotic pressure (Π). Below the point of zero turgor the cells showed a linear decrease in volume with increase in external osmotic pressure. The volume at zero turgor was taken to be V_0. The volume of the cell at the osmotic pressure of PBS i.e., under the condition of compression testing was taken to be V. Eq. (1) was then used to find the initial stretch ratio for that cell.

The mean initial stretch ratio for the whole cell population was also measured by Mastersizer and was found to be 1.07 ± 0.04 (95% confidence limits; 10^4 measurements), reasonably consistent with the visualization chamber data.

3.4. Fluorescent microscopy

Yeast cells were stained with WGA-Alexa 488 and fluorescence microscopy was used to measure bud scar number and size (Table 1). In a mixed population, it was observed that approximately 50% of the cell population was daughter cells, 25% 1 scar cells, 12.5% 2 scar cells and 12.5% the remainder. These ratios are reasonable as the number of cells doubles with each division. It should be noted that about half of the cells in stationary phase cultures are daughter cells; cell age and culture time should not be conflated.

The equivalent spherical diameter and aspect ratio increased with the number of bud scars, consistent with earlier findings (Powell et al., 2003). The mean equivalent spherical diameter was found to be 5.10 ± 0.10 μm, after adjustment for the proportion of cells of each type. This agrees well with the value from the Mastersizer of 5.07 ± 0.04. The mean aspect ratio was found to be 1.16 ± 0.01, greater than 1.09 found earlier for rehydrated Fermipan yeast cells (Smith et al., 1998). There was a significant difference between the mean equivalent spherical diameter of mother cells and daughter cells, and also their mean aspect ratios.

3.5. Cell sorting by FACS

FACS was used to sort WGA-Alexa488 stained cells with 0, 1, 2, and 3 or more bud scars according to fluorescence intensity. The purity of the daughter cell fraction was 100%, single-scarred cells were found to be approximately 90% pure and two-scarred cells were found to be approximately 65–70% pure. The impurities were mainly partially-budded cells, which were discernable during compression testing and could therefore be discarded. The fraction with 3 or more bud scars was also 100% pure.

3.6. Cell wall thickness

The wall thickness of a cell cannot be measured in current compression testing equipment. It was assumed by earlier workers (Smith et al., 2000b; Stenson et al., 2011) and in this study that the wall thickness (at zero turgor) is in a fixed ratio, τ, to the cell radius. As in previous work, this ratio was determined for the whole population by transmission electron microscopy,

Table 1
Major and minor axis lengths of WGA-Alexa488 stained cells measured by fluorescent microscopy with respect to number of bud scars. The aspect ratio is the ratio of the major to the minor axis length. One hundred cells per fraction; 95% confidence limits. (The population values were calculated assuming the unsorted cells were 50% daughter cells, 25% 1 scar cells, 12.5% 2 scar cells and 12.5% cells with 3 or more scars.)

Number of bud scars	Major axis length (μm)	Minor axis length (μm)	Equivalent spherical diameter (μm)	Aspect ratio
0	4.7 ± 0.2	4.1 ± 0.1	4.3 ± 0.1	1.13 ± 0.01
1	6.2 ± 0.1	5.1 ± 0.1	5.5 ± 0.1	1.21 ± 0.01
2	6.7 ± 0.2	5.6 ± 0.2	5.9 ± 0.2	1.20 ± 0.02
≥3	7.5 ± 0.1	6.4 ± 0.1	6.8 ± 0.1	1.18 ± 0.02
Population mean	5.7 ± 0.1	4.8 ± 0.1	5.1 ± 0.1	1.16 ± 0.01

Table 2
Corrected cell wall thickness and cell radius with respect to number of bud scars. (The population values were calculated assuming the unsorted cells were 50% daughter cells, 25% 1 scar cells, 12.5% 2 scar cells and 12.5% cells with 3 or more scars.)

Number of bud scars	Number of cells measured	τ	Measured cell radius (μm)	Corrected cell radius (μm)	Measured cell wall thickness (nm)	Corrected cell wall thickness (nm)
0	21	0.057 ± 0.004	1.9 ± 0.1	2.3 ± 0.1	220 ± 10	131 ± 5
1	19	0.041 ± 0.003	2.4 ± 0.1	2.9 ± 0.1	211 ± 6	119 ± 5
2	19	0.047 ± 0.005	2.3 ± 0.1	2.9 ± 0.1	230 ± 15	134 ± 5
≥ 3	12	0.021 ± 0.002	2.6 ± 0.2	3.1 ± 0.2	135 ± 5	68 ± 4
Population mean		0.047 ± 0.004	2.2 ± 0.1	2.6 ± 0.1	209 ± 9	121 ± 5

Table 3
Summary of cell size data by four measurement methods applied to the whole population. NA means that this measurement is not available for the specified method. (Errors are 95% confidence limits).

Method	Mastersizer	Fluorescence microscopy	TEM	Compression testing
Mean equivalent spherical diameter (μm)	5.07 ± 0.04	5.1 ± 0.1	5.3 ± 0.2	NA
Mean minor axis length (μm)	NA	4.8 ± 0.1	NA	4.8 ± 0.1
Mean major axis length (μm)	NA	5.6 ± 0.1	NA	NA

independently to compression testing. In this study, the ratio was found separately for each sorted cell fraction, as shown in Table 2. This shows how τ varied with the number of bud scars. There were no significant differences between the cell wall thicknesses of cells with less than 3 bud scars, including daughter cells. Cells with three or more bud scars showed low values of τ and relatively thin cell walls. However, given the low numbers of such cells, these data may not be reliable. Overall, the correction factor from measured to actual cell wall thickness was 0.57. (This value has been adjusted for the proportion of cells in each fraction by number of scars in the unsorted sample i.e., 50:25:12.5:12.5 for 0, 1, 2 and 3 or more scars, respectively). This is close to the value of 0.6 presented by Smith et al. (2000b). The corrected method of finding τ (Supplementary information) has a small but not negligible effect on calculated wall thickness. It should be noted that both methods assume cells are spherical, which is not quite correct in practice, as shown in Table 1. The effect of errors or changes in wall thickness values on elastic modulus estimates is discussed later. Table 3 summarises cell size data, as determined by Mastersizer, fluorescence microscopy and TEM. Compression testing data are also included and will be described later. The values seem to be internally consistent.

3.7. Compression testing

Direct measurements obtained by compression testing are the cell size, the bursting force and the deformation at bursting. The cell size was a measure of the minor axis length of the generally ellipsoidal yeast cells (because cells lie with their major axis parallel to the horizontal base of the chamber). The values agreed well with the direct measurement of the same parameter by fluorescence microscopy (Table 3). This suggests that the cell size measured by compression testing is realistic.

In a preliminary trial, compression tests were conducted on both stained and unstained cells (unsorted) to check for any effect of staining on the mean bursting force and deformation at bursting. No significant differences were observed. This is consistent with the fact that the stain cannot penetrate the yeast cell wall due to its high molecular weight (Yamamoto et al., 1981) and its specific binding to *N*-acetyl-D-glucosamine in bud scars (Powell et al., 2003). It was reasonable to assume that differences between mechanical properties of mother and daughter cells was not an artefact of staining. Table 4 shows compression testing data for each cell fraction. The cell size (mean minor axis length) gradually increased with the number of scars, which is consistent with the observation that cells get larger as they age (Lesage and Bussey, 2006; Powell et al., 2003). For all fractions, the bursting force was independent of cell size (data not shown), confirming earlier findings for whole cell populations (Mashmoushy et al., 1998; Smith et al., 2000b). The force at bursting was also independent of the number of bud scars. Meanwhile, the mean % deformation at bursting gradually decreased with the number of scars. The population means for the bursting force and the % deformation at bursting were significantly lower than previous values found using rehydrated dried cells (Stenson et al., 2011), even if allowance were made for the different proportions of each type of cell in those measured here and the unsorted sample). This might be because of differences in culture media (not known for dried Fermipan) or might be an effect of drying on cell membranes and walls.

Table 4
Comparison of the mean minor axis length, the mean bursting force and the mean % deformation at bursting for sorted yeast cells. (Errors are 95% confidence limits).

Number of bud scars	Number of cells measured	Mean minor axis length (μm)	% Deformation at bursting	Bursting force (μN)
0	24	4.1 ± 0.2	58 ± 3	81 ± 8
1	55	5.1 ± 0.1	54 ± 1	95 ± 4
2	59	6.0 ± 0.1	54 ± 1	104 ± 6
≥ 3	63	6.7 ± 0.1	46 ± 1	80 ± 6
Overall	201	5.7 ± 0.1	52 ± 1	91 ± 3

The mean bursting force and the mean % deformation at bursting were independent of storage time over 3 weeks at 4 °C (data not shown).

Bursting force and deformation at bursting are not intrinsic mechanical properties of yeast cells as they depend on factors such as cell wall thickness. It is therefore necessary to model cell behaviour mathematically to extract useful parameters, in particular the elastic modulus of the wall and some failure criteria, as described in Section 2. The model was that of Stenson et al. (2009). As described earlier, this previously successful model could be fitted to force deformation data up to cell bursting for 69% of cells overall and only 32% of daughter cells. Possible explanations were that the cells were not spherical, as assumed by the model, that the incompressibility assumption was violated, and/or the cell walls were not linear elastic to cell bursting.

The sphericity assumption was not strictly true for the rehydrated Fermipan yeast cells of previous work (Stenson, 2008) and is even less correct for the cultured cells of this study, with a population mean aspect ratio of 1.16 (Table 1). Although it was not possible to measure cell aspect ratios during compression testing (because of poor quality images), force–deformation traces give values of the minor diameters of cells. The mean values were similar for those cells to which the model could be fitted and for the remainder i.e., 4.8 ± 0.1 μm (Table 3) against 4.7 ± 0.1 μm, respectively. It was concluded that non-sphericity was probably not the cause of model failure. Nevertheless, there might have been effects from this on model parameter estimation. However, it is arguable that the initial shape becomes of lesser significance at high deformations, when the cell wall is very stretched in all tangential directions.

It is difficult to measure hydraulic conductivity of yeast cells directly and this was not attempted but compression testing showed no significant difference in mean elastic modulus or mean initial stretch ratio for compression speeds of 68 μm s^{-1} and above. This agrees with the findings of Stenson et al. (2011) for Fermipan. If the incompressibility assumption was invalid, changes with compression speed might be expected. Furthermore, it seems unlikely that the cultured cells of this study were more permeable than the rehydrated Fermipan yeast cells of previous work (Stenson, 2008). The incompressibility assumption seems reasonable in the circumstances.

It was eventually hypothesised that some cell walls were probably not linear elastic. It is not clear why this would be nor why daughter cells were a particular problem in this respect. However, it is known that (small) daughter cells do not contain detectable amounts of chitin (Schekman and Brawley, 1979) and are not stained by Calcafluor White (De Nobel et al., 1990) nor labelled by WGA-gold (Shaw et al., 1991). Perhaps this is the basis of the difference in elastic behaviour. In any case, it is remarkable that any natural material shows linear elastic behaviour over the very large deformations, as has been shown for the majority of cells studied in this work, previously for other cultured cells (Smith et al., 2000b) and for rehydrated Fermipan yeast cells (Smith et al., 2000b; Stenson et al., 2009, 2011).

Considering only those cells which could be modelled successfully, the elastic modulus and the stretch ratio of the walls were found from the model (Table 5). It can be seen that the mean elastic modulus for the cells that could be analysed was 300 ± 20 MPa (201 cells, 95% confidence limits) whilst the mean initial stretch ratio was 1.05 ± 0.01. There was an expected variability in the mean elastic moduli and the value for cells with three or more scars is as unreliable as the cell wall thickness estimate upon which it was based, as described earlier. The important distinction with respect to scars was again between daughter and mother cells i.e., those without a bud scar or those with any number of scars. The mean elastic modulus was lower for daughter cells (170 ± 20 MPa, 24 cells) with a higher mean initial stretch ratio (1.07 ± 0.02, 24 cells) than for mother cells (320 ± 20 MPa and 1.04 ± 0.01 for 177 cells). The differences were significant at the 5% level. These data suggest that bud scars make yeast cell walls stiffer, which is consistent with atomic force microscopy measurements showing that scars are significantly stiffer than normal yeast cell walls (Touhami et al., 2003). However, each bud scar only occupies around 1–2% of the cell surface and one might not expect the effect on global cell wall properties to be large. Furthermore, there does not seem to be an identifiable dependence of the modulus on the number of scars. An alternative explanation is that daughter cells contain no detectable chitin in their walls, as mentioned earlier, whereas walls of mother cells contain 0.1% to 0.2% chitin (dry weight) excluding scars and up to 2% including scars (Klis et al., 2002). It is possible the chitin has a significant effect on the wall mechanical properties even at apparently low levels. It is not possible to decide this matter from the information available in this study.

It should be noted that it may be more appropriate to use a surface rather than the elastic modulus to describe the mechanical properties of the cell wall (Smith et al., 2000b; Stenson et al., 2011). The surface modulus is the product of the elastic modulus and the cell wall thickness and appears directly in the model, with the elastic modulus found from it using a mean wall thickness (Stenson et al., 2009). The difficulty of measuring accurately cell wall thicknesses supports the use of the surface modulus as a more reliable measure. However, it is not clear if the surface modulus has any relevance to cell disruption. Nevertheless, the values are given in Table 5. Once again it may be seen that the crucial distinction is between daughter and mother cells with the latter having significantly higher surface moduli on average.

The bursting force given in Table 4 is not an intrinsic mechanical property of the cells, as its value will depend on the compression method. For the 69% of cells that could be fitted to bursting assuming a linear elastic cell wall, it was possible to calculate failure criterion such as the stresses and strains at failure. The model showed that the stresses and strains were highest in the circumferential direction at the equator and it was therefore assumed that cell bursting was controlled by these parameters. The principal circumferential Hencky strains and Cauchy stresses at the equator were calculated (Stenson et al., 2009, 2011) as shown for each type of cell in Table 6. It can be seen that the mean circumferential strain at bursting decreased with scarring (consistent with stiffer walls) whilst the stress increased (0.37 ± 0.04 and 86 ± 8 MPa, respectively for daughter cells; 0.27 ± 0.01 and 109 ± 5 MPa, respectively for mother cells). Overall it appears that bud scars make yeast cell walls stronger as well as stiffer. As one might have expected some stress

Table 5
Mean wall elastic moduli and mean initial stretch ratios for yeast cells separated by number of bud scars. The population values were calculated assuming the unsorted cells were 50% daughter cells, 25% 1 scar cells, 12.5% 2 scar cells and 12.5% cells with 3 or more scars.

Number of bud scars	Number of cells modelled	% Non-linear elastic cells	Mean elastic modulus (MPa)	Mean initial stretch ratio	Surface modulus (Nm^{-1})
0	24	67	170 ± 20	1.07 ± 0.01	19 ± 3
1	55	23	290 ± 20	1.04 ± 0.01	29 ± 2
2	59	20	190 ± 10	1.05 ± 0.01	26 ± 2
≥ 3	63	12	460 ± 30	1.04 ± 0.01	30 ± 2
Mother cells only	177	18	320 ± 20	1.05 ± 0.01	29 ± 1
Overall Population	201	43	300 ± 20	1.05 ± 0.01	28 ± 1
	–	–	230 ± 20	1.06 ± 0.01	24 ± 2

Table 6
Circumferential stress and strain at failure and strain energy per unit volume at failure. Errors are 95% confidence limit.

Number of bud scars	Number of cells modelled	Circumferential stress at failure (MPa)	Circumferential strain at failure	Strain energy per unit volume at failure (MPa)
0	24	86 ± 8	0.37 ± 0.04	19 ± 3
1	55	110 ± 5	0.29 ± 0.02	17 ± 2
2	59	78 ± 4	0.29 ± 0.01	12 ± 1
≥ 3	63	138 ± 8	0.23 ± 0.01	17 ± 2
Mother cells (with scars)	177	109 ± 5	0.27 ± 0.01	16 ± 1

concentration near a bud scar, this suggests that the major influence on the strength might be chitin in mother cell walls.

Besides the presence of bud scars on some cells, lack of cell sphericity (Table 1) implies the cell walls are not isotropic and homogeneous, which is an assumption of the model. It is clear that this model assumption was usually violated in practice. Nevertheless, the modelling has allowed significant differences between the mechanical properties of mother and daughter cells to be identified and suggests strongly that the number of scars on mother cells is not an important determinant of those properties. This needs further investigation. One possibility would be the further use of finite element analysis that would allow the easy incorporation in the modelling of non-linear elastic cell wall behaviour and non-sphericity of cells. It might also be possible to incorporate or at least investigate the role, if any, of bud scars in the overall stiffness and strength of the walls.

4. Conclusion

Compression testing by micromanipulation on FACS sorted Baker's yeast cells has indicated for the first time that there is a difference in mechanical properties of daughter and mother yeast cells. It is not clear if this was a direct effect of the scars, which are stiffer than normal cell wall (Touhami et al., 2003), or because normal mother cell walls contain chitin (Takagi et al., 1983). The latter explanation is favoured here (without direct evidence).

Cell sorting by FACS is a useful method for investigating yeast cell wall mechanics and Alexa Fluor 488 conjugated WGA results in clear staining of scars to allow such sorting. However, the current model of yeast cell compression is not adequate for cultured yeast cells, despite its earlier success (Stenson et al., 2011), because cultured cells are not spherical and some show non-linear elastic cell wall behaviour. Other methods such as finite element analysis will be required for further investigations.

Notation

V	Cell volume μm^3
V_0	Cell volume at zero turgor μm^3
λ_s	Initial stretch ratio
τ	Ratio of cell wall thickness to cell radius

Acknowledgements

The BD FACSAria2 cell sorter was purchased with the support of UK Biotechnology and Biological Sciences Research Council REI grant BB/F011237/1.

Appendix A. Supporting information

Supplementary data associated with this article can be found in the online version at http://dx.doi.org/10.1016/j.ces.2012.08.027.

References

Aguilar-Uscanga, B., Francois, J.M., 2003. A study of the yeast cell wall composition and structure in response to growth conditions and mode of cultivation. Lett. Appl. Microbiol. 37, 268–274.

Arfsten, J., Leupold, S., Bradtmöller, C., Kampen, I., Kwade, A., 2010. Atomic force microscopy studies on the nanomechanical properties of *Saccharomyces cerevisiae*. Colloids Surf., B 79, 284–290.

Berner, J.L., Gervais, P., 1994. A new visualization chamber to study the transient volumetric response of yeast cells submitted to osmotic shifts. Biotechnol. Bioeng. 43, 165–170.

Bitterman, K.J., Medvedik, O., Sinclair, D.A., 2003. Longevity regulation in *Saccharomyces cerevisiae*: linking metabolism, genome stability and heterochromatin. Microbiol. Mol. Biol. Rev. 67, 376–399.

Champluvier, B., Kamp, B., Rouxhet, P.G., 1989. Immobilization of β-galactosidase retained in yeast: adhesion of the cells on a support. Appl. Microbiol. Biotechnol. 27, 464–469.

Chen, C.Y., Dewaele, S., Braeckman, B., Desmyter, L., Verstraelen, J., Borgonie, G., Vanfleteren, J., Contreras, R., 2003. A high-throughput screening system for genes extending life-span. Exp. Gerontol. 38, 1051–1063.

De Nobel, J.G., Klis, F.M., Priem, J., Munnik, T., Van den Ende, H., 1990. The glucanase-soluble mannoproteins limit cell wall porosity in *Saccharomyces cerevisiae*. Yeast 6, 491–499.

Freifelder, D., 1960. Bud position in *Saccharomyces cerevisiae*. J. Bacteriol. 124, 511–523.

Klis, F.M., Boorsma, A., de Groot, P.W.J., 2006. Cell wall construction in *Saccharomyces cerevisiae*. Yeast 23, 185–202.

Klis, F.M., Mol, P., Hellingwerf, K., Brul, S., 2002. Dynamics of cell wall structure in *Saccharomyces cerevisiae*. FEMS Microbiol. Rev. 26, 239–256.

Lesage, G., Bussey, H., 2006. Cell wall assembly in *Saccharomyces cerevisiae*. Microbiol. Mol. Biol. Rev. 70, 317–343.

Mashmoushy, H., Zhang, Z., Thomas, C.R., 1998. Micromanipulation measurement of the mechanical properties of Baker's yeast cells. Biotechnol. Tech. 1, 925–929.

Mercadé-Prieto, R., Nguyen, B., Allen, R., York, D., Preece, J.A., Goodwin, T.E., Zhang, Z., 2011. Determination of the elastic properties of single microcapsules using micromanipulation and finite element modelling. Chem. Eng. Sci. 66, 2042–2049.

Nobel, P.S., 1969. The Boyle van't Hoff relationship. J. Theor. Biol. 23, 375–379.

Powell, C.D., Quain, D.E., Smart, K.A., 2003. Chitin scar breaks in aged *Saccharomyces cerevisiae*. Microbiology 149, 3129–3137.

Powell, C.D., Van Zandycke, S.M., Quain, D.E., Smart, K.A., 2000. Replicative ageing and senescence in *Saccharomyces cerevisiae* and the impact on brewing fermentations. Microbiology 146, 1023–1034.

Schekman, R., Brawley, V., 1979. Localized deposition of chitin on the yeast cell surface in response to mating pheromone. PNAS 76, 645–649.

Shaw, J.A., Mol, P.C., Bowers, B., Silverman, S.J., Valdivieso, M.H., Duran, A., Cabib, E., 1991. The function of chitin synthase-2 and synthase-3 in the *Saccharomyces cerevisiae* cell cycle. J. Cell Biol. 114, 111–123.

Sinclair, D.A., Mills, K.A., Guarente, L., 1998. Aging in *Saccharomyces cerevisiae*. Annu. Rev. Microbiol. 52, 533–560.

Smith, A.E., Moxham, K.E., Middelberg, A.P.J., 1998. On uniquely determining cell wall material properties with the compression experiment. Chem. Eng. Sci. 53, 3913–3922.

Smith, A.E., Moxham, K.E., Middelberg, A.P.J., 2000a. Wall material properties of yeast cells: Part II. Analysis. Chem. Eng. Sci. 55, 2043–2053.

Smith, A.E., Zhang, Z., Thomas, C.R., 2000b. Wall material properties of yeast cells: Part 1 Cell measurements and compression experiments. Chem. Eng. Sci. 55, 2031–2041.

Stenson, J.D., 2008. Investigating the Mechanical Properties of Yeast Cells. Ph.D. Thesis, The University of Birmingham, United Kingdom.

Stenson, J.D., Hartley, P., Wang, C., Thomas, C.R., 2011. Determining the mechanical properties of yeast cell walls. Biotechnol. Progr. 27, 505–512.

Stenson, J.D., Thomas, C.R., Hartley, P., 2009. Modelling the mechanical properties of yeast cells. Chem. Eng. Sci. 64, 1892–1903.

Takagi, A., Harashima, S., Oshima, Y., 1983. Construction and characterization of isogenic series of *Saccharomyces cerevisiae* polyploid strains. Appl. Environ. Microbiol. 45, 1034–1040.

Touhami, A., Nysten, B., Dufrene, Y.F., 2003. Nanoscale mapping of the elasticity of microbial cells by atomic force microscopy. Langmuir 19, 4539–4543.

Wang, C.X., Pritchard, J., Thomas, C.R., 2006. Investigation of the mechanics of single tomato fruit cells. J. Texture Stud. 37, 597–606.

Werner-Washbourne, M., Braun, E., Johnston, G.C., Singer, R.A., 1993. Stationary phase in the yeast *Saccharomyces cerevisiae*. Microbiol. Rev. 57, 383–401.

Yamamoto, K., Tsuji, T., Matsumoto, I., Osawa, T., 1981. Structural requirements for the binding of oligosaccharides and glycopeptides to immobilized wheat germ agglutinin. Biochemistry 20, 5894–5899.